

Interactions between hyphae of the filamentous fungus *Podospora anserina*.

Alice Nappa

April 2024

Contents

1	Intro/Abstract	2
2	Meeting induced branchings	2
2.1	Introduction to MIBs	2
2.2	Sons born after fusion and nature of the mother	2
2.3	Summary of Apical and Lateral growth characteristics	3
2.3.1	Apical branches	3
2.3.2	Lateral branches	3
2.3.3	Apical/Lateral latency time	4
2.4	Phase diagram	4
2.4.1	Branching rates	6
3	Behaviour of an hypha approaching an obstacle	8
3.1	Introduction of interaction with the obstacle	8
3.2	Functions settings	8
3.2.1	Obstacles' identification	8
3.2.2	Distance	9
3.2.3	Tangent function	9
3.3	Avoidment identification algorithm	9
3.3.1	Tuning of vision code parameters	9
3.3.2	Image cleaning	10
3.3.3	Step by step	11
3.4	Avoidment dataset analysis	11
3.4.1	Spontaneous avoidment	11
3.4.2	Distances	11
3.4.3	Phase plot $\delta\theta$ vs δv_{\perp}	11
3.5	Speed analysis	13
3.5.1	Old and young branches	15
3.5.2	Vector representation	16
3.6	Stopping	17
3.7	Fusion	18

1 Intro/Abstract

During their growth, fungi can create very dense and complex network. There are no observations in nature of simple structures, but it is still not clear why the growth of the single branches evolves the way it does. In this work, we exploit the digital reconstruction on the mycelial network of *Podospora anserina* to analyze some of the typical behaviour of a free tip approaching a pre-existent hypha (obstacle). In particular, we identified 5 different behaviours (figure 1): Avoidment (1b), fusion/meeting (1e), stopping (1a), overlaps (1c), and meeting induced branching (2). First in chapter 2, it will be introduced the MIB (*Meeting Induced Branching*) phenomena. The first aim was to understand if the phenomena existed and if its properties are attributed to the normal hypha growth process or not. If the second option is verified, we thus try to characterize the phenomena characteristics.

Secondly in chapter 3, we analyzed the others possible behaviours (fig. 1b, 1a, 1e) of a hyphae in presence of an obstacle, and tried to characterize the outcomes of the interaction through parameters as the angles between directions, orthogonal speed and distance between branches. The initial hypothesis to verify is the existence of a sort of "attraction law" among branches that causes the branches to curve their trajectories, overlap or fuse during their growth.

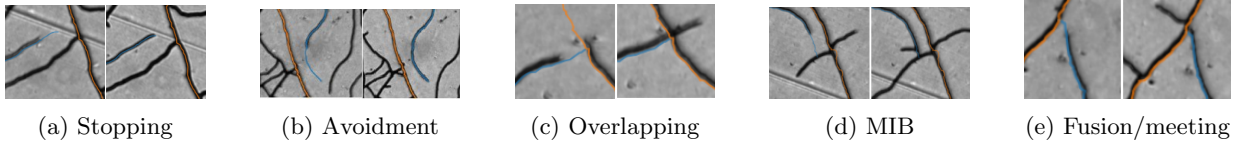


Figure 1: Main typical behaviours

2 Meeting induced branchings

Vedi files:

MIB_FOR_APICAL_LATERAL_MOTHERS_CUMULATIVE_FIT_EXP_MIB_BRANCHING_RATIO_PHASE
DIAGRAM_NEWNEW

2.1 Introduction to MIBs

What we mean by *Meeting induced branchings* is the phenomena where a growing branch ending in fusion (*Mother branch*), at a time later than fusion, starts to grow some outgoing neighbours. The question we address is: does this process happen according to typical branching rules or is it a different process? We will report the branching properties of apical and lateral branches and we will start the analysis by trying to understand if the phenomena is anyhow influenced by the nature of the mother or of the son, or both. After, we will give the mathematical characterization of the phenomena in the phase plot $\Delta T, \Delta L$ and prove that MIBs not only exist but they are also not matching with usual growing description present in literature.

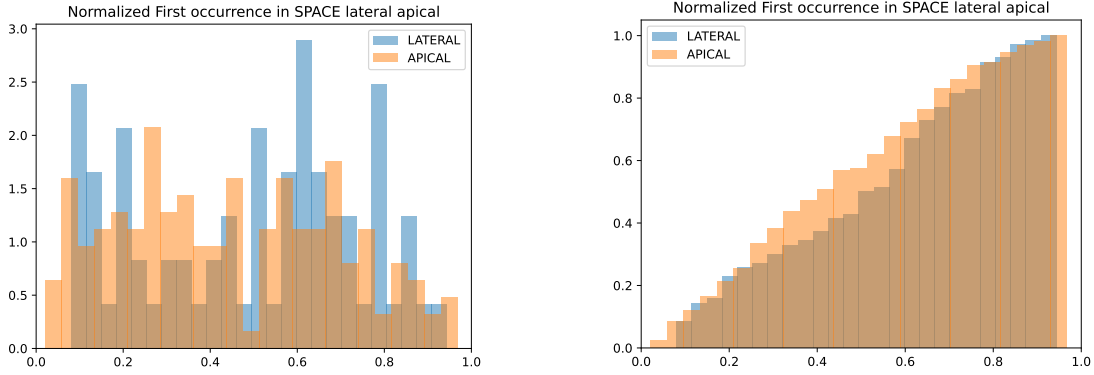
2.2 Sons born after fusion and nature of the mother

Our MIB characterization started considering as MIB any kind of branch, coming from any kind of mother, whose growth is starting on the mother branch, after its fusion.

Let's start counting how many cases we have into consideration so see if the numbers are significative or not. In the reseau there are 957 APICAL branches, and a total of 421 cases of MIB on 165 different branches.

So the 17,24% of Apical Branches presents MIB. Accordingly, in the reseau there are 926 Lateral branches, and a total of 140 cases of MIB spread on 70 different branches. So the 7,5% of Lateral Branches presents MIB.

We tried to understand first of all if the nature of the mother (Apical/Lateral) had an influence on the manifestation of the phenomena. Despite the difference in counts of sons, in figure ?? we can see the cumulative distributions of the normalized (with respect to the length of the mother branch) first occurrence in distance with respect to the fusion node, and comparing the distributions with a Kolmogorov-Smirnov test statistic we obtain a $p - value = 0.18$, and setting a probability reference as $\alpha = 0.05$ we can easily declare that the two distributions are alike and thus there is no difference in the position on the mother branch in which MIB start to appear. We will see below that indeed there is difference in the branching rate.



(a) Distribution of the ΔL distance from fusion point and position on the mother of the first emerging MIB

(b) Cumulative distributions of 2a to analyze the test statistics on it.

2.3 Summary of Apical and Lateral growth characteristics

So far we considered MIBs to be simply sons growing after fusion of the mother branch. In this section we are going to expand the concept extending the definition considering the theory underlying known apical and lateral branching processes.

2.3.1 Apical branches

The key factor in the growth of **Apical branches** is the SPK; the SPK is mainly composed of an accumulation of secretory vesicles at the apex; as the hypha stops growing, the SPK disappears. In general we will assume that apical branches are distributed following an exponential law with respect to the apex of the mother branch and constant growth speed. According to this description of apical growth, we thus believe that after the stopping of the mother branch there can't be any new branch growing on it. If we verify the presence of Lateral or Apical son branches growing after the stopping of the mother branch, the mechanism of growth of these latters can't be regulated by SPK as the mother. With no further details for now we will consider that all the branches not obeying normal branching rules can be considered as potential MIBs, so apical "forbidden" branches.

2.3.2 Lateral branches

While the growth speed of the apical branches can be considered approximately constant from the moment of branching onwards, the underlying assumption characterizing **Lateral growth** is that the branch reaches its stationary speed after a latency time τ_{AL} . Infact, the branching probability is uniform on the hypha except for a forbidden zone close to the apex, it can thus be modeled as a sigmoid. The rest of the dynamics is however not accessible to the extent that the apex end up meeting another hypha, thus putting an end to the monitoring. So in this case we will consider, as will be explained in detail below, that there are some

”allowed” lateral branches that respect the expected latency time, and the ”forbidden” ones growing before, will be defined MIBs.

2.3.3 Apical/Lateral latency time

MIBs occur after fusion, so in theory there shouldn't be apical MIBs.

Let's analyze the lateral case in more detail. If the growth after fusion follows the same rules as the normal case, branchings are allowed to occur after a $\Delta\tau_{AL}$ waiting period between the first passage of the mother branch in the branching node and the actual growth start moment.

Moreover, we assume uniform growing speed. The magnitudes of quantities of interest are reported below:

- $v_{ap} \simeq 4 \mu m/min = 45 pixels/frame$
- $v_{lat} \simeq 2.9 \mu m/min = 32.63 pixels/frame$
- $\Delta\tau_{AL} \simeq 5 frames$

Following the lateral branching description given before, let's define L_{MIB} the branching forbidden zone on the mother hypha close to the apex. It is a dynamic quantity whose evolution is given from the law:

$$L_{MIB}(iT) = v_{AP/LAT} \cdot (\Delta\tau - iT) \quad (1)$$

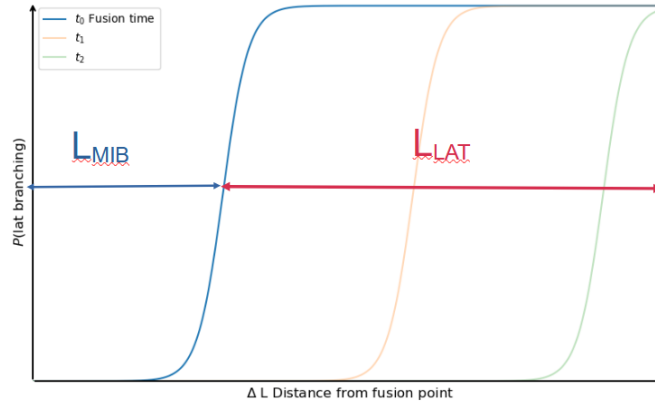


Figure 3: Branching probability of lateral sons. t_0, t_1, t_2, \dots refer respectively to fusion time and 1st, 2nd, ... frame after fusion time.

The point $P_{LAT} = 1/2$ moves with the speed of the mother branch v_{LAT} or v_{AP} according to its nature. The blue region L_{MIB} is the forbidden region in the natural branching process: so if there are branches born in that region they must come from another branching process and those are the ones that we will identify as MIBs. In summary, MIBs are either those born after fusion of apical mother or branches that live in the forbidden region L_{MIB} .

2.4 Phase diagram

Let's select the points belonging to MIBs as illustrated in 2.3.3. The first point of the analysis is to understand if these points exist or not, and whether they do, to characterize the phenomena.

Points are selected using the following algorithm:

1. Find all the branches of the réseau ending in fusion. Separate them according to their Apical or Lateral nature. These branches are *mother branches*.

2. For all mothers, create the list of “*outgoing neighbors*” \iff all branches whose starting node belongs to mother branch. These branches are *son branches*. Also sons are separated according to their nature.
3. Among all sons, we will chose the ones whose starting time is posthumous to the fusion of the mother.
4. Among sons selected in steps 1-3 we take those whose coordinates belong to MIB region.

All points selected according to **steps 1-3** of the algorithm are reported in figure 4, for each son after fusion it is scattered $\Delta T, \Delta L$, respectively distance in time and space from the fusion node.

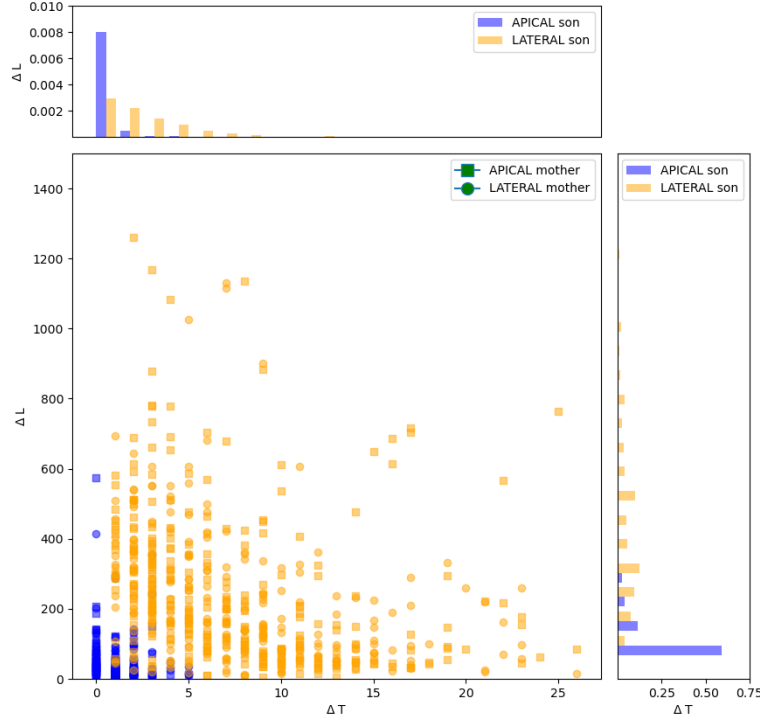


Figure 4: Phase diagram with separation Apical/Lateral mother and son

First, we can observe that points labeled with squares and circles do not create a phase separation in the phase diagram ΔL vs ΔT . From now on we can thus neglect the information about the nature of the mother.

In **step 4** we take for each point the two corresponding coordinates and see if it belongs or not to the L_{MIB} region spanning between x axes and the line $L_{MIB}(iT) = v_{AP/LAT} \cdot (\Delta\tau - iT)$. This procedure is explained in figure 5.

Taking into consideration only first occurrences for illustration, we select MIBs as the points below the blue line for apical mothers and orange one for lateral mothers: basically almost all those who stay in the L_{MIB} region except for the two apical sons visible in figure staying between the two lines.

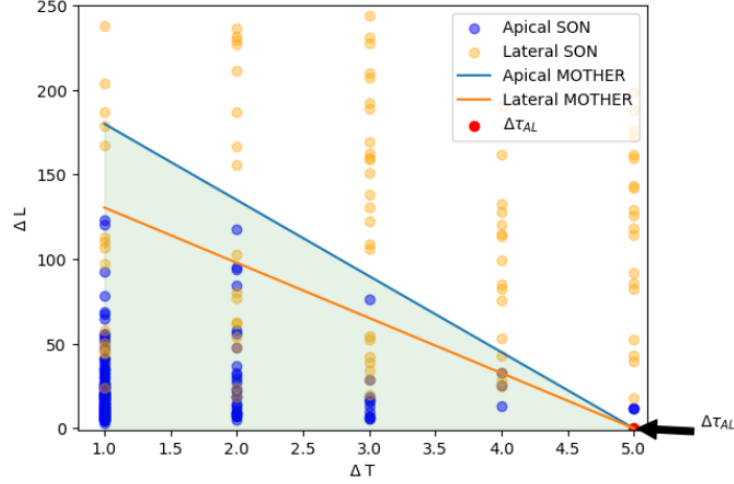


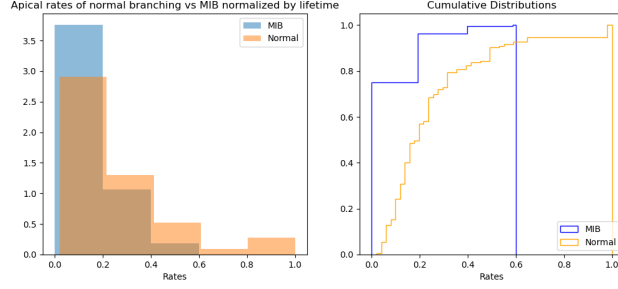
Figure 5: Phase diagram with separation Apical/Lateral mother and son

The existence of points in the phase diagram belonging to the forbidden region for now gives a first proof of the existence of MIBs. To further characterize the hypothesis that they don't obey traditional branching laws, in the following section it will be analyzed the branching rates of these branchings and compared to normal ones.

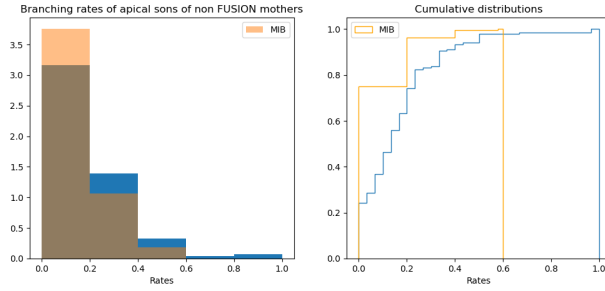
2.4.1 Branching rates

The phenomenological apical/lateral distinction is linked to a lower growing rate in the case of lateral branchings. We will thus take into consideration apical branching rates only (there are very little lateral MIBs in the network in analysis so we neglect them for this last step). The aim is to compare the MIBs branching rates to those of normal apical branches, in this case analyzing the branching rates defined as number of MIBs / branch lifetime.

We firstly compute the branching ratios for all the apical mothers of MIBs before they fuse and compare to the MIBs ones after fusion. This comparison is done in fig. 6a, while in fig. 6b the comparison is made with the distributions of branching rates of any apical branch.



(a) Comparison between apical branching rates of normal branching process and MIB branching process for branches that produce MIB before and after fusion.



(b) Comparison between apical branching rates of normal branching process and MIB branching process for any branch, that undergo fusion and not.

What we can observe is first of all that MIBs on a given branch are present with typically 1,2 or 3 occurrences, while there are more sons in normal branches. Secondly, comparing the distributions with a Kolmogorov test statistics, we obtain a $p - value \approx 10^{-10}$ implying thus a strong statistical difference in the distributions, furtherly confirming our initial hypothesis of exitance of MIBs and of different branching characteristics.

3 Behaviour of an hypha approaching an obstacle

3.1 Introduction of interaction with the obstacle

By simple observation of the network one can notice that branches are in general not moving straight on a radial direction. Most of them, indeed, can take on the most jagged trajectories. There is no answer yet why the trajectory is not straight. What we want to prove here is that the closeness to an obstacle can influence the trajectory of apexes by attracting or repelling them. Indeed, in presence of an obstacle we will classify the behaviour according to whether the apex change its trajectory, whether fuse on it, either stop before reaching it.

In general, the avoidment of an obstacle is called *autotropism* (positive or negative whether the branch is attracted or repelled). The aim of this section is to first analyze the growth behaviour changes in presence of the obstacle, then try to understand if there is a way to discriminate the nature of the interaction (attractive/repulsive). In general we will collect datas for 3 types of events (Stopping, Fusion/Meeting and Avoidment) to create a dataset of θ, d_{\perp} and v_{perp} and look for eventual correlations among these values.

3.2 Functions settings

3.2.1 Obstacles' identification

Being intrested in the interactions among branches, we shall thus implement an algorithm to identify, for a given branch at a given time, its obstacles.

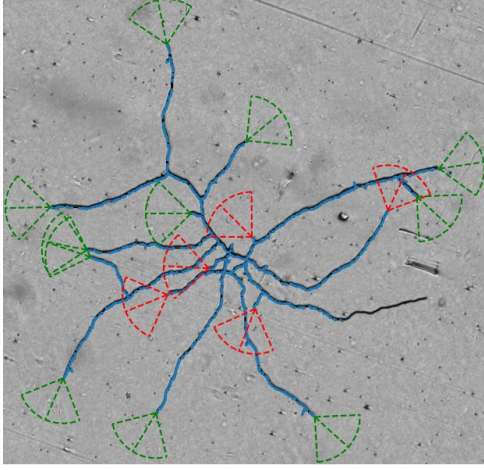
First of all we shall define what is an obstacle.

Let's create, around a moving tip, a vision cone of r_{min} radius of it and α its width. We can say that if the vision cone is occuppied (occupied \iff the coordinates of any node of any branch are within its area at a given time) then that branch at that time "has an obstacle".

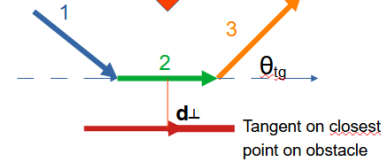
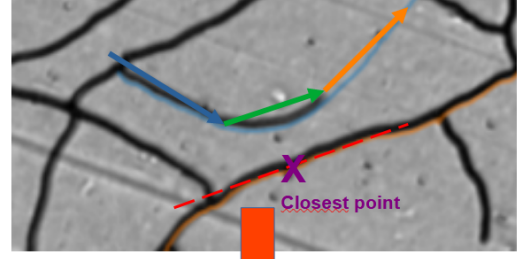
$$\text{Branch has an osbtacle} \iff \text{any node of any branch} \in \text{vision cone area}$$

The function we implemented places every existing node on a grid. For each instant of time t we calculate the list of all free apexes where an apex is considered free if it is a degree 1 node and the time . We implemented a function returning, given a radius and an angle identifying a vision cone for the growing tip, if that cone was occupied from another branch or not, returning T / F lists as shown in (7a). Moreover we can know who are the (closest) neighbors occupying the path, at what distance (d_{\perp}) they are placed, and the projections of the speed of the growing branch with respect to the obstacle, namely v_{\perp} and $v_{//}$.

This analysis was limited to branches having more than 25 nodes, because very small branches grow in very narrow regions and result to have a large number of neighbors, therefore making it hard to identify which branch is causing what behaviour.



(a) Reseau at $t = 20$ frames. **Occupied** and **obstacle-free** branches.



(b) Geometry of vectors in closest distance point in the couple branch-obstacle.

Figure 7: Neighbors selection and data collection when an obstacle is close.

3.2.2 Distance

To identify the points of closest distance between obstacle and branch it is calculated the matrix of distances among all nodes of the branch and all nodes of the obstacle and taken the smallest. Once identified the nodes of closest distance, we calculate the line passing from the node on the branch and orthogonal to the tangent on the obstacle. See figure 7.

3.2.3 Tangent function

The tangent function on the obstacle is calculated taking the closest distance couple of nodes branch-obstacle and from the node on the obstacle, calculating the unit vector passing from the node after and before of the closest distance one. See figure 7.

3.3 Avoidment identification algorithm

We will arbitrarily define an avoidance the case of a branch whose speed vector turns of at least an angle α_{lim} and during the turning see an obstacle. The intersection of these two datasets returns what we imagine as "avoidment". The procedure for obstacles identification has been explained already in 3.2.1. The procedure to find turning branches is reported below.

Let α_{lim} be the minimum angle that the speed vectors have to form to be considered an avoidance. Since avoidments have the more different curvature radiuses, let's define by $\alpha_{i,i+1}$ the angle that the vector velocity i of that branch makes with $i + 1$. We impose on the latters:

$$\text{Deviation of trajectory} \iff \alpha_{i,i+1} > \alpha_{lim} \quad OR \quad \alpha_{i,i+2} > \alpha_{lim}$$

3.3.1 Tuning of vision code parameters

Deciding at what distance or not something is defined an obstacle is arbitrary. From (aggiungi citazione tesi clara) the avoidance typical distance is considered to be $r_{min} = 62.5\mu m$. We imposed a $r_{min} \approx$ network radius and collected the distributions of the closest distances in figure 8. Thus we will choose as parameters of the vision cone $r_{min} = 100\mu m$ and the angle of the cone is varied $\theta \in \pi/2, \pi/3, \pi/4, \pi/6$

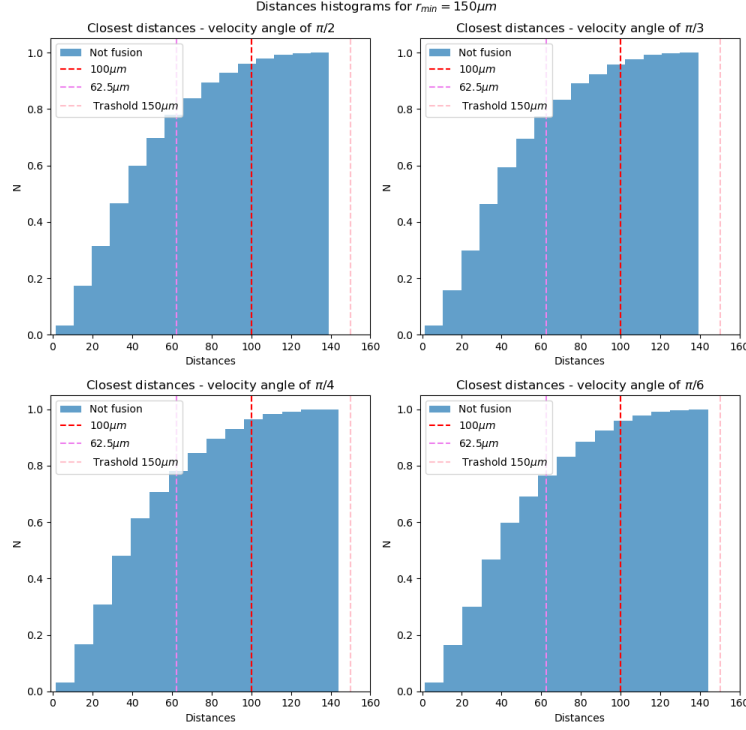


Figure 8: Cumulative of distributions of closest obstacles' distances with a $r_{min} \gg 1$

The figures show that there is no difference in the distributions of minimum distances varying on the angle θ of the vision cone, so we arbitrarily set a value of $\theta = \pi/2$. Moreover, we put in this simulation a very big radius but the extremal value of the distribution is $\sim 140 nm$ meaning that for every branch the closest obstacle is at maximum $\sim 140 nm$

3.3.2 Image cleaning

All the branches that we managed to identify as avoidance can be visualized, and by eye I could spot that there was a repeated bug in the creation of the branches for which some MIBs resulted in my avoidance dataset. To avoid this problem, we performed an image screening of the dataset. For each couple Branch-Obstacle, we take a small screenshot of the two branches in correspondence of the closest point. Applying an imaging filtering method that topologically identifies how many components the figure is made of, we deleted the 1-piece couples (if the figure is made of one only piece it means that the obstacle and the branch are united and so no avoidance is happening) and retained only the > 2 pieces couples.

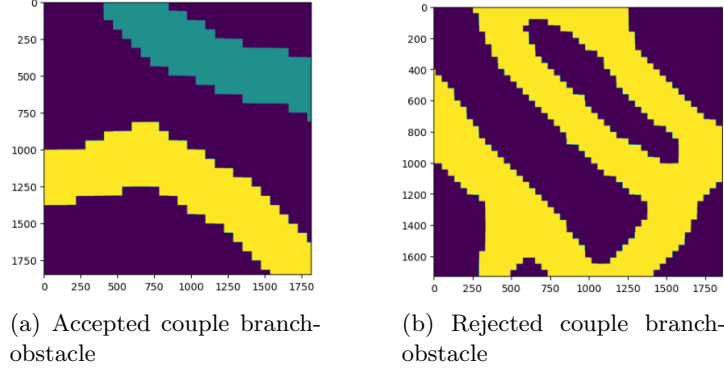


Figure 9: Respectively accepted and rejected couples branch-obstacle

3.3.3 Step by step

1. First of all we create the dataset of all branches that see an obstacle (closest).
2. After we create independently the dataset of all branches that deviate trajectory in their path as described in ??.
3. We intersecate the two datasets following:

Does it turn?

3.4 Avoidment dataset analysis

3.4.1 Spontaneous avoidance

To address the velocity deviation phenomena to the attraction caused from another hyphae we can check what is the ratio of spontaneous direction reorientation compared to the cases of obstacle-caused speed reorientation. In the table 1 there are reported the numbers in consideration. "Errors" refers to any datation problem, speed not defined problems etc. "Common nodes" are the couples branch-obstacle that share a node, it is thus impossible to define a minimum distance and use the functions we created.

	KeyErrors	Nodes in common	Tot Couples	Valid	Spont Re-or
RESEAU 16	277	160	716	272	7
RESEAU 17	330	433	1230	432	35
RESEAU 04	329	150	1185	422	284

Table 1: Number of datapoints in our dataset to explude the hypothesis of spontaneous re-orientation

3.4.2 Distances

3.4.3 Phase plot $\delta\theta$ vs δv_{\perp}

To create this plot, let's take the instant of minimum distance and calculate our coordinates θ, d_{\perp} and v_{\perp} for 5 point: the minimum distance one, two before, two after. For these we calculate the $\delta_{i+1,i}$ so we obtain, for each avoiding branch, a dataset of 4 points: $\delta_{12}, \delta_{23}, \delta_{34}, \delta_{45}$. The plot 10 is showing them all together (for reseau 17 but they look all alike) and one by one in 11:

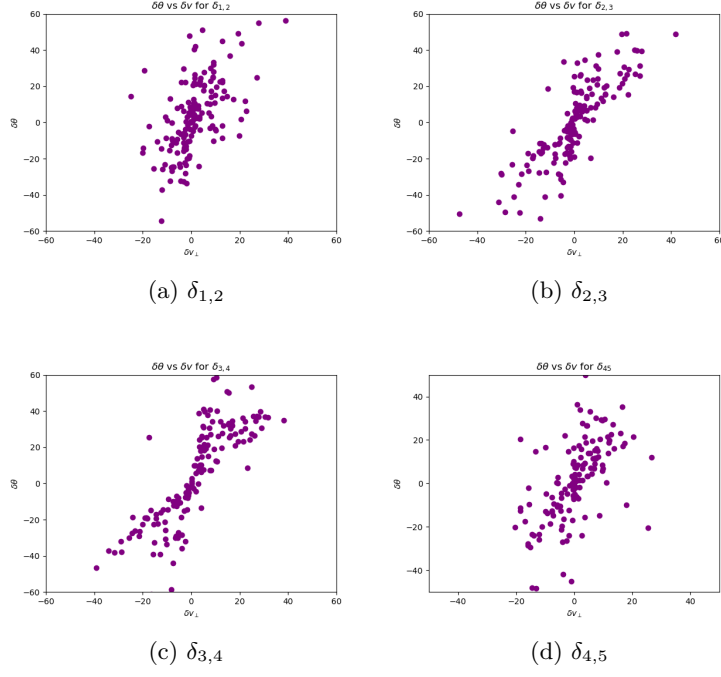


Figure 11: Plot of $\delta\theta$ vs δv_{\perp} for $\delta_{i+1,i}$, $i \in 1, \dots, 5$

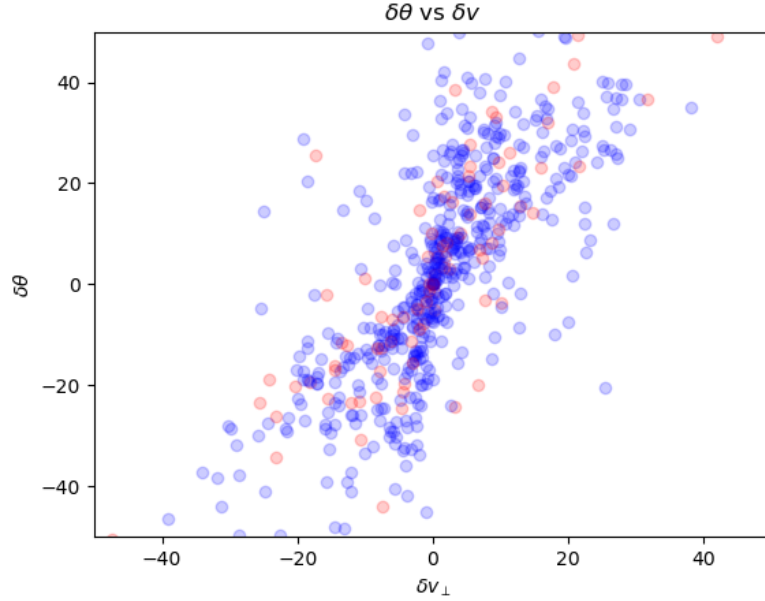


Figure 10: Scatter plot of all $\delta_{i,i+1}$ for all branches of $\delta\theta$ vs δv_{\perp} , in red **apical** branches in blu **lateral**

From a first glance one can notice two things:

- The scatter plot gets very aligned when closing up to the obstacle.
- The majority of avoiding branches doesn't get too close to the obstacle, at a borderline distance of $\approx 10 \text{ pixels}$.

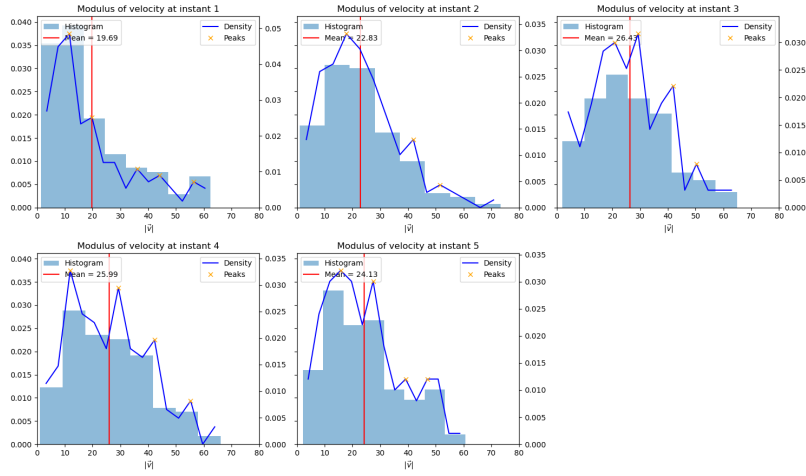
- The positiveness or not of theta depends by the direction of approach of the branch (if it is along the normal or against it).

The "cone" that the speeds create could have been addressed to the apical and lateral difference, but as very clearly shown in **metti ref grafico** it is not that causing the difference. Let's thus proceed with speed analysis to check what happens to the speed when coming closer to the obstacle.

3.5 Speed analysis

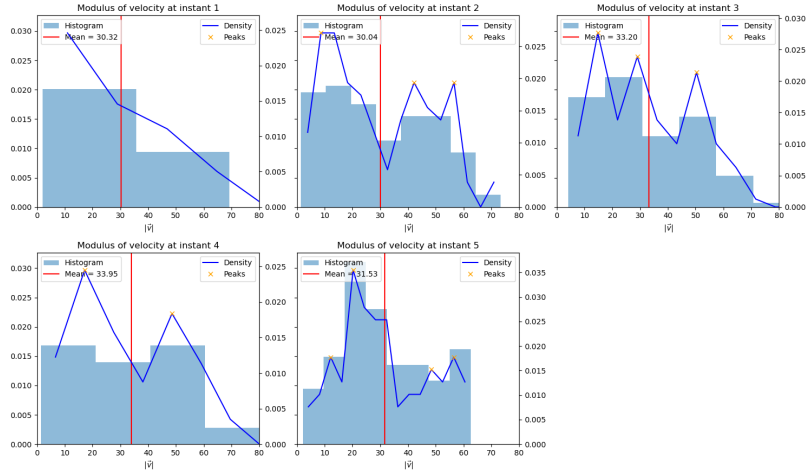
For each instant considered ($t = 1, \dots, 5$) we average the speeds for all branches. So the $t = i, i \in 1, \dots, 5$ plot refers to the average of the magnitude of all the i -th speed vector, for each branch. As there is a clear split in the graph, according to speed, we want to study the distributions of speed to check if there is any emerging bimodal to which we can address the dual speeds.

Histograms of Modulus of Velocity at Different Instants



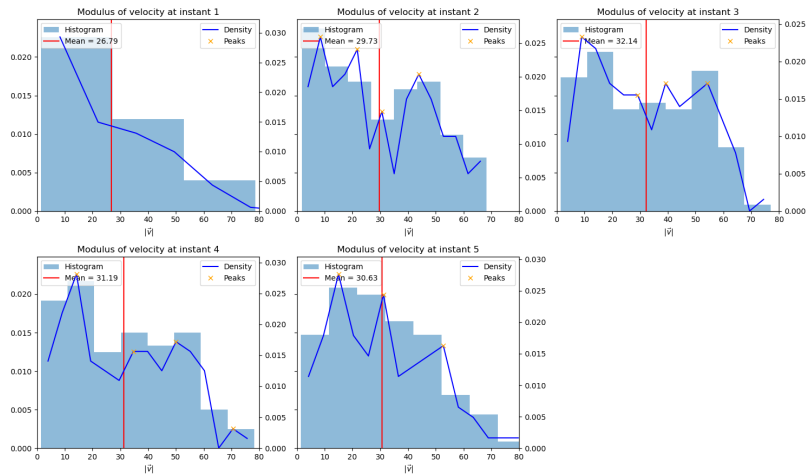
(a) Histogram of velocities for reseau 04

Histograms of Modulus of Velocity at Different Instants



(b) Histogram of velocities for reseau 16

Histograms of Modulus of Velocity at Different Instants



(c) Histogram of velocities for reseau 17

Figure 12: Histogram of speed module for each instant 1, ..., 5

As shown in 12 the speed distribution in the closest point is almost bimodal in all the networks as expected and the module of speed is not only not constant in all the networks, but it's increasing in the vicinity of the obstacle.

In addition it can be noticed a "shifting" of the peak and a redistribution of velocities as we approach the third histogram (third one is the closest distance one), after which the distribution tends to go back at its original shape.

3.5.1 Old and young branches

Since it's now clear the presence of a double behaviour induced from the obstacle in the speeds, we now want to understand what is the cause of duality, since it's clearly not addressable to apical and lateral distinction.

Let's suppose that the branch is avoiding the obstacle with constant speed. For simple trigonometry reasons:

$$v_{\perp} = v \cdot \sin(\theta)$$

assuming v is constant:

$$\begin{aligned} \frac{\partial v_{\perp}}{\partial \theta} &= v \cdot \cos(\theta) \quad \rightarrow \quad \delta v_{\perp} = v \cdot \cos(\theta) \cdot \delta \theta \\ &\rightarrow \delta v_{\perp} = v \cdot \sqrt{1 - \left(\frac{v_{\perp}}{v}\right)^2} \cdot \delta \theta. \end{aligned} \quad (2)$$

We find a relation linking the variation of orthogonal speed to the variation of the angle. The approximation of constant speed is approximately true close to the obstacle, and in that neighborhood $v_{\perp}/v \approx 0$ so that we obtain the relationship:

$$\delta v_{\perp} = v \cdot \delta \theta \quad \rightarrow \quad \delta \theta = \frac{1}{v} \cdot \delta v_{\perp} \quad (3)$$

Meaning that the angular coefficient (multiplied by a radiant - degrees conversion factor) is the inverse of a speed that characterizes the behaviour of the hyphae in the closest point distance.

What we know is that apical branches, from the moment of their birth, need **quanti** timeframes to reach asymptotic speed, while lateral ones take ~ 8 frames. Let's assume that "young" and "old" branches behave differently close to the obstacle.

The distinction between old and young branches can be made according to $\Delta t_{avoiding} = age(branch) - t_{start}(branch)$ if $\Delta > 8$ frames the branch will be considered old, young otherwise. Coloring in blue the old branches and in red the young ones, and projecting everything in the first quadrant of the plot (without changing the information content of the plot) we plotted $\delta \theta$ vs δv_{\perp} for $\delta_{2,3}$.

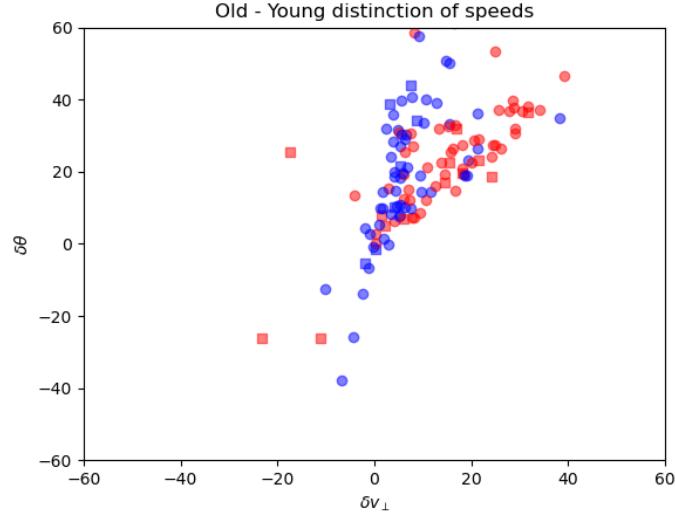


Figure 13: $\delta\theta$ vs δv_{\perp} for $\delta_{2,3}$ with **young** / **old** distinction.

Let's try to fit singularly the plots to obtain an estimation of the typical speeds.

3.5.2 Vector representation

Let's plot, to understand if there exist a directionality of the interaction with the obstacle, a vector representation in which:

- For the 4 $\delta_{i,i+1}$ instants.
- Bottom of the arrow is the point $(\delta\theta, v_{\perp})$
- Tip of the arrow is $(\theta + \delta\theta, v_{\perp} + \delta v_{\perp})$

The same graph has been done also for the case of fusion, in which there is no average directionality of the vectors and the mean is 0.

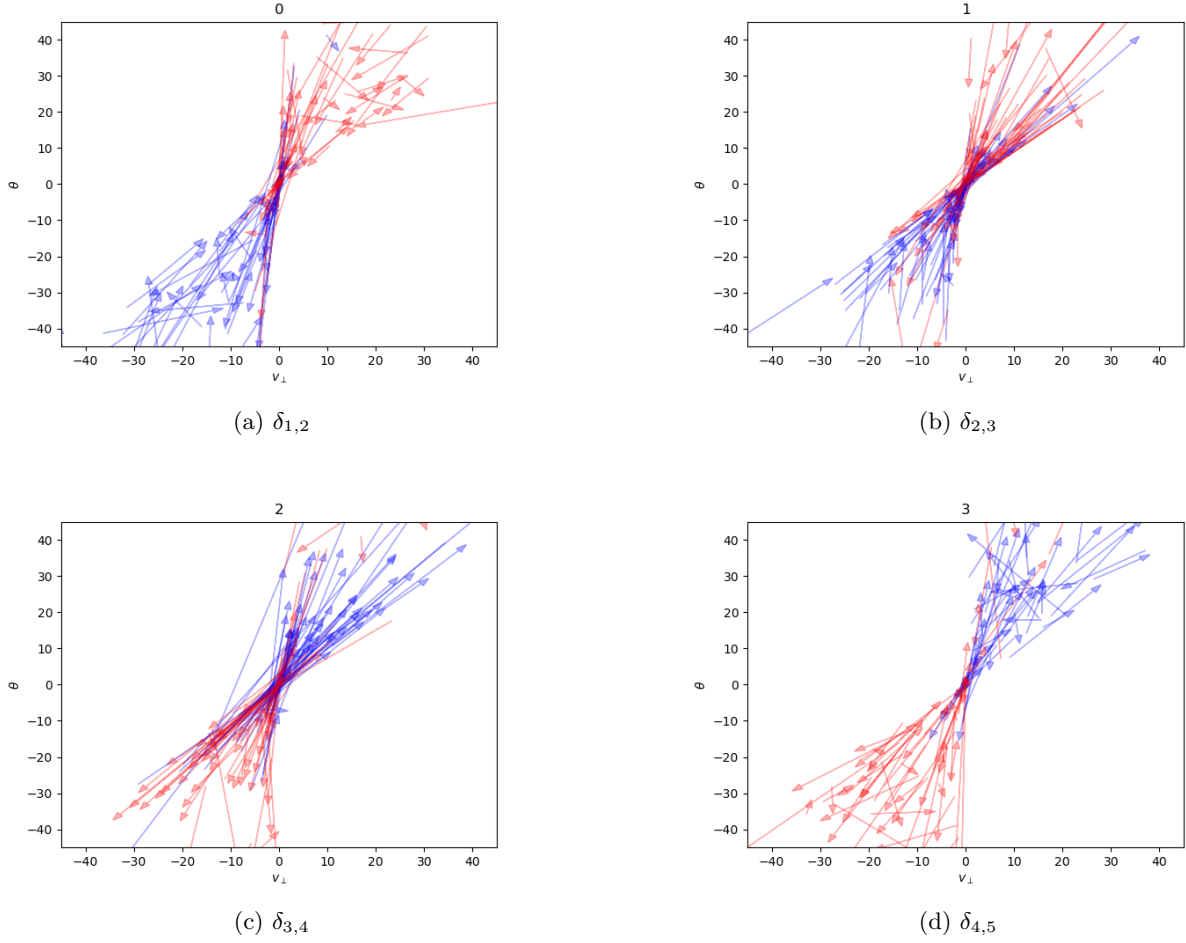


Figure 14: Plot of $\theta + \delta\theta$ vs $v_{\perp} + \delta v_{\perp}$ for $\delta_{i+1,i}$, $i \in 1, \dots, 5$

In this case the first quadrant represents attraction moment, and the negative one repulsion. As we can see at the first and last instant everything is chaotic and there is no preferred directionality of the variation of the vector. In the closest distant points, not only there is directionality but it changes behaviour: at first the deviation pushes toward the 0 point of the graph (0 is the parallel to obstacle position), after, passing from 0, there is repulsion and the vectors push to unalign with the obstacle.

3.6 Stopping

The same analysis was also addressed to stopping dataset. The difference between a stopping and a complete avoidance is difficult to define, indeed the dataset is very small compared to others and the avoidance dataset is composed of some ambiguous branches. However, typically, by observation, one can notice that stopping can happen before or after alignment. If the point of minimum distance branch-obstacle is also the ending point of the branch we will call this a stopping and not an avoidance.

In general we will look for branches whose last node is degree 1 and see an obstacle at that time, moreover the ending time of the branch must be earlier than the ending time of the resau.

For only 25 datapoints, we collected the minimum distance and the orthogonal speed, and compared it to the avoidance case in ??

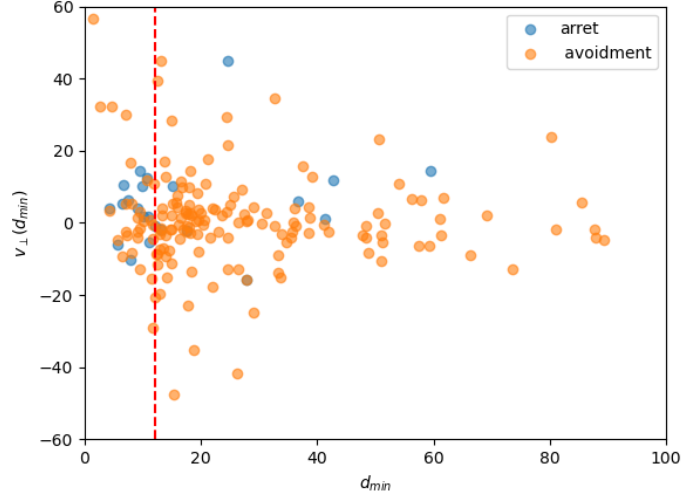


Figure 15: v_{\perp} calculated in the minimum distance point vs d_{min} .

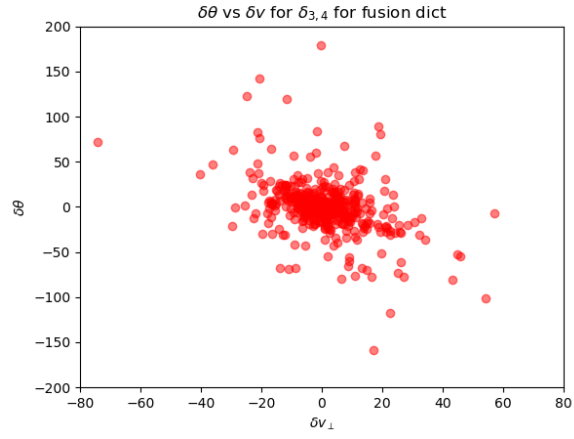
As we can expect, the values of v_{\perp} for the stopping are smaller than in the avoidance case. Moreover, the scatters for all the networks make us think that stopping branches arrive closer to their obstacle than branches who avoid it. In red there is the line at $d_{min} = 10px$, an orientative estimation by eye to the distance separating the two phenomenas. I will not report the scatter plot $\delta\theta, \delta v_{\perp}$ since there is no emerging correlation in this case.

3.7 Fusion

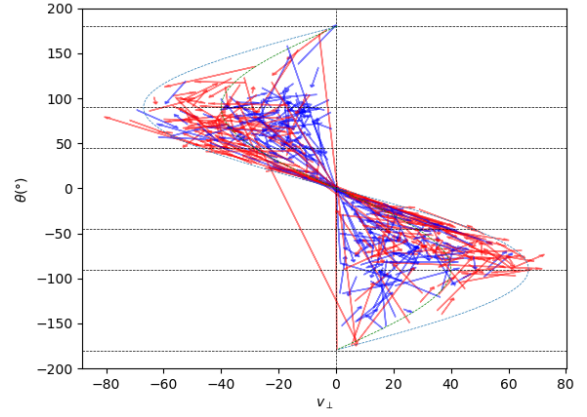
By fusion we mean, as shown in figure 1e, the encounter between two branches, whether it is anastomosis or overlap.

We took for this dataset all of the branches that end by "fusion" on their obstacle. We did not go deeper in checking if the fusion happens immediately after seeing the obstacle, at the end of the lifetime etc.. In general we will consider branches that encounter with their own obstacle.

For these branches we collected the usual collection of coordinates θ, v_{\perp} ; of course minimum distance is not defined in this case. For trigonometric reasons of course we were expecting $v_{\perp} \propto \sin(\theta)$. As shown in 16b the proportionality holds, not obviously, also for the coordinates $v_{\perp} + \delta v_{\perp}$



(a) $\delta\theta$ vs δv_{\perp} for **fusion**



(b) Plot of θ vs v_{\perp} at closest distance time. The arrow points towards the point $(v_{\perp} + \delta^{3,4}v_{\perp}, \theta + \delta^{3,4}\theta)$. blue is old branches , red is youngers.